Direct Observation of the Complex Formation of GDP-Bound Transducin with the Rhodopsin Intermediate Having a Visible Absorption Maximum in Rod Outer Segment Membranes†

Takefumi Morizumi, Hiroo Imai, and Yoshinori Shichida*

Department of Biophysics, Graduate School of Science, Kyoto University, Kyoto 606-8502, Japan, and CREST, Japan Science and Technology Agency, Japan

Received March 11, 2005; Revised Manuscript Received May 26, 2005

ABSTRACT: Rhodopsin is a photoreceptive protein that is present in rod photoreceptor cells, inducing a GDP−GTP exchange reaction on the retinal G-protein transducin (Gt) upon light absorption. This exchange reaction proceeds through at least three steps, which include the binding of photoactivated rhodopsin to GDP-bound Gt, the dissociation of GDP from the rhodopsin−Gt complex, and the binding of GTP to the nucleotide-unbound Gt. These steps have been thought to occur after the formation of the rhodopsin intermediate, meta-II; however, the extra formation of meta-II, which reflects the formation of a complex with Gt, was inhibited in the presence of excess GDP. Here, we use a newly developed CCD spectrophotometer to show that a meta-II precursor, meta-Ib, which has an absorption maximum at visible region, can bind to Gt in its GDP-bound form in urea-washed bovine rod outer segment membranes. The affinity of meta-Ib for GDP-bound Gt is about two times less than that of meta-II for GDP-unbound Gt, indicating that the extra formation of meta-II is observed at equilibrium even in the presence of the meta-Ib−Gt complex. This is the first identification of a complex that includes the GDP-bound form of G protein. Our results strongly suggest that the protein conformational change of the rhodopsin intermediate after binding to Gt is important for the induction of the nucleotide release from the α-subunit of Gt.

The visual transduction process in photoreceptor cells begins with light absorption by rhodopsin, a member of the G-protein-coupled receptor family which contains a light-absorbing chromophore, 11-*cis*-retinal (*1*). Light initiates cis−trans isomerization of the chromophore, inducing the conformational change of rhodopsin's protein moiety to form an activated rhodopsin state (*2*−*4*). This state then triggers a G-protein-mediated signal transduction cascade that eventually generates electrical responses in the photoreceptor cells (*5*, *6*). The 11-*cis*-retinal bound in the protein moiety of the rhodopsin acts as an inverse agonist, suppressing the spontaneous activation of rhodopsin, while all-*trans*-retinal acts as an agonist (*7*). Rhodopsin is thus a G-protein-coupled receptor whose intrinsic inverse agonist converts to an agonist upon light absorption.

To date, several intermediate states of rhodopsin have been identified to occur during the bleaching process. Among these intermediates, the metarhodopsin II (meta-II), which forms an equilibrium state with its precursor metarhodopsin I (meta-I) (*8*), is thought to be crucial for G-protein activation (*9*). In the presence of transducin (Gt),[1] the equilibrium shifts in favor of meta-II, indicating that the meta-II forms a complex with Gt (*10*, *11*). The excess meta-II formed in the presence of Gt is called extra-meta-II, and its formation is abolished in the presence of GTP (*9*). Meta-II can thus form a complex with Gt in the absence of GTP, dissociating from Gt through the GDP−GTP exchange reaction (Gt activation) in the presence of GTP. It is noteworthy that extra-meta-II formation is also abolished in the presence of GDP (*12*), suggesting that Gt, which forms the complex with meta-II, is in a nucleotide-unbound form (empty form) and that the binding of the guanine nucleotide to Gt causes complex dissociation. Since Gt in its resting state is in a GDP-bound form, prior to forming the complex with meta-II there would exist a state other than meta-II that could bind to the GDP-bound form of Gt.

We previously discovered an intermediate state that formed prior to meta-II and interacted with Gt (*13*−*15*). We called this intermediate state meta-Ib, because it exhibits an absorption maximum about 20 nm blue shifted from that of the previously identified meta-I (now known as meta-Ia). Figure 1 illustrates the rhodopsin reaction scheme, including both meta-Ia and meta-Ib. We found that meta-Ib could bind to Gt and did not induce a GDP−GTP exchange reaction (*13*−*15*). However, because of the limited time resolution of our spectroscopic techniques, we could only identify this intermediate state by using low-temperature spectroscopy and a detergent-solubilized rhodopsin−glycerol mixture. Therefore, the identification of this intermediate under the physiological conditions and the elucidation of its characteristics distinct from those of meta-II are important for a better understanding of the molecular mechanism of G-protein activation by rhodopsin.

In the present study, we developed a cooled CCD spectrophotometer with a time resolution of 9.7 ms to identify

† This work was supported in part by Grants-in-Aid for Priority Area and a Grant for Biodiversity Research of the 21st Century COE (A14) from the Japanese Ministry of Education, Culture, Sports, Science, and Technology to Y.S. and H.I.

* To whom correspondence should be addressed at Kyoto University. Phone: +81-75-753-4213. Fax: +81-75-753-4210. E-mail: shichida@vision-kyoto-u.jp.

[1] Abbreviations: Gt, retinal G-protein transducin; Gtα, α-subunit of transducin; GPCR, G-protein-coupled receptor; ROS, rod outer segment; GTPγS, guanosine 5′-*O*-(3-thiotriphosphate).

10.1021/bi0504512 CCC: $30.25
Published on Web 06/30/2005

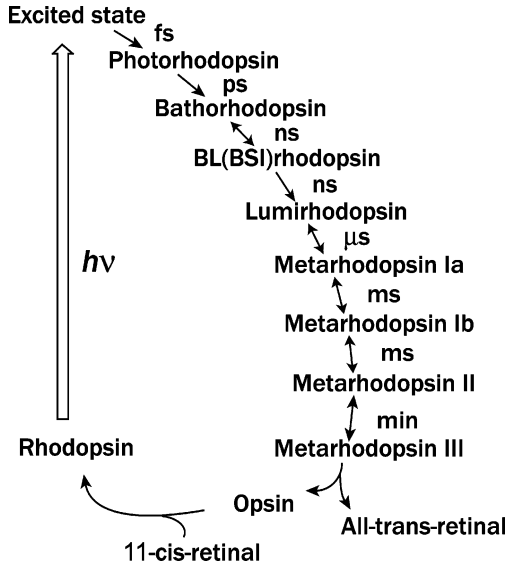

FIGURE 1: Photobleaching process of bovine rhodopsin (*43*−*46*). The time domains of the transitions between intermediates observed at room temperature are shown to the right of the arrows.

meta-Ib in rod outer segment (ROS) membranes at physiological temperature. The results showed that meta-Ib exists under physiological conditions. It was also found that meta-Ib interacts with Gt even in the presence of excess GDP such that extra-meta-II was no longer formed. These results suggest that meta-Ib is a physiologically relevant intermediate that interacts with Gt in a manner different from that of meta-II. The EC_{50} value of meta-Ib binding to Gt (in the presence of GDP) was estimated to be two times larger than that of meta-II binding to Gt (in the absence of GDP). The Hill coefficients are approximately 2 in both cases. The high-affinity (low EC_{50} value) binding of meta-II to Gt can account for the formation of extra-meta-II in the presence of Gt, even with the existence of an interaction between meta-Ib and Gt. On the basis of these results, we will discuss the activation mechanism of Gt by rhodopsin intermediates.

MATERIALS AND METHODS

Preparation of Urea-Stripped Bovine Rod Outer Segment Membrane and Gt. Using a standard discontinuous sucrose gradient method, rod outer segments (ROS) were isolated from frozen bovine retinas (*16*). The ROS membranes were then treated with 3 M urea (pH 8.0) and were repeatedly washed with a low ionic strength buffer (pH 7.2) to remove membrane-associated proteins, such as Gt and PDE, as previously described by Shichi et al. (*17*). The washed membranes were stored at −80 °C until they were to be used. Gt was prepared from bovine ROS membranes following the method described by Fukada et al. (*18*). Gtα-GTPγS was prepared using GTPγS instead of GTP, according to the method of Phillips and Cerione (*19*). The concentration of intact Gt was determined by fluorometric titration, as described by Fahmy and Sakmar (*20*).

The membrane samples suspended in buffer (30 mM NaCl, 60 mM KCl, 2 mM $MgCl_2$, 1 mM dithiothreitol, and 40 mM MOPS, pH 7.0 at 4 °C) were sonicated on ice at low power (dial was set to 3 of 10) in nitrogen for 90 s with a sonicator (Ultrasonic W-220). This was done to diminish turbidity. The ROS samples containing 7.5 μM rhodopsin were then subjected to spectroscopic measurements.

Time-Resolved Spectroscopy. We recorded absorption spectra using a CCD spectrophotometer that was specially constructed in collaboration with Hamamatsu Photonics Co., Ltd. This spectrophotometer is able to continuously record the spectra (700−300 nm) with a wavelength resolution of 1.6 nm in time intervals of 9.7 ms. Rhodopsin bleaching in the sample caused by monitoring light was about 1.85% after 100 spectra recordings, which is comparable to that observed in a commercial spectrophotometer, such as the Shimadzu MPS 2000 spectrophotometer. The sample temperature was regulated to within 0.1 °C by a temperature controller (Neslab RTE-111) that was attached to the sample cell holder. The sample was then irradiated with a 532 nm light pulse (∼5 ns) from a YAG laser (Hoya continuum) 100 ms after the measurements began.

Spectral Analysis. The spectral recording obtained after rhodopsin irradiation was composed of spectral components of meta-Ia, meta-Ib, meta-II, rhodopsin unreacted, and isorhodopsin produced by photoreaction of intermediates (*14*). The percentages of intermediates in the sample at selected times after irradiation were estimated by comparing the sample spectrum with the spectra of three intermediates after subtracting the spectra of the residual rhodopsin and isorhodopsin from the sample spectrum. The absolute spectra of three intermediates are estimated as follows.

To estimate the meta-Ib spectrum, we compared the spectral region at wavelengths that were longer than 450 nm of the difference spectrum between meta-Ib and meta-II (Figure 2B, inset). This was done using a template spectrum derived by Lamb (*21*) and Govardovskii et al. (*22*) as a parameter of the absorption maximum. The best-fitted spectrum was considered to be the meta-Ib spectrum. The meta-II spectrum was obtained by adding the meta-Ib spectrum to the difference spectrum between meta-Ib and meta-II (the sign was reversed). To estimate the meta-Ia spectrum, the spectrum of the mixture of the three intermediates (Figure 5C) was compared with those of meta-Ib, meta-II, and the template spectrum whose maximum was set as a parameter. The best-fitted spectrum was then considered to be the meta-Ia spectrum. Because the meta-Ia spectrum was influenced by the contaminating lumirhodopsin (lumi) intermediate (*23*), the meta-Ia maximum was located around 500 nm and varied with the sample temperatures (505 nm at 4 °C and 498 nm at 37 °C). According to Govardovskii et al. (*22*), the β-band amplitudes of these spectra were fixed at 26% of those of the α-bands. To determine the equilibrium constants, the molar extinction coefficients of these intermediates were assigned according to Applebury (*24*).

RESULTS

Interactions of Rhodopsin Intermediates with Gt. The spectroscopic data obtained by the newly developed CCD spectrophotometer are shown in Figure 2A. Rhodopsin in the sonicated ROS membranes (curve 1 in Figure 2A) at 4 °C exhibited an absorption maximum of about 500 nm. A blue shift of the spectrum was caused by irradiation with a laser pulse (curve 2 in Figure 2A). We observed an absorbance increase at about 380 nm with a concurrent decrease at about 480 nm (curves 2−11 in Figure 2A). Eighteen seconds after irradiation (curve 11 in Figure 2A), spectral changes were apparently complete, indicating the formation of an equilibrium state. The enlarged spectral

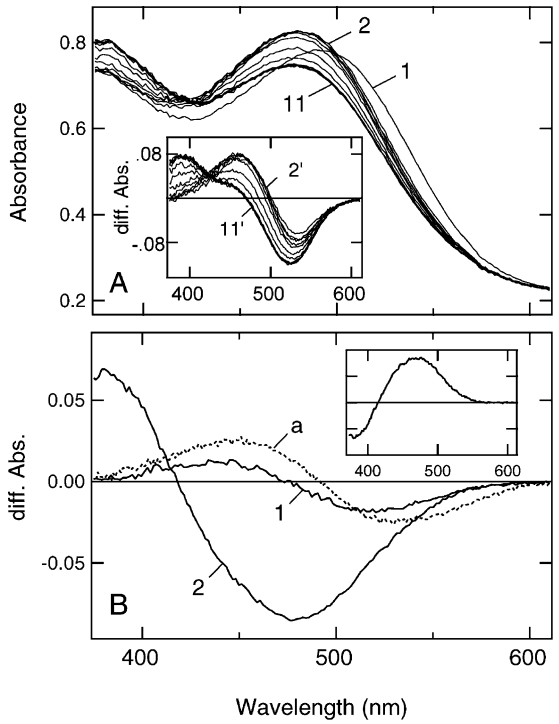

FIGURE 2: Formation of meta-Ia, meta-Ib, and meta-II by irradiation of rhodopsin in ROS with a 532 nm laser pulse at 4 °C. (A) Spectral changes observed after irradiation of rhodopsin in ROS membranes with a 532 nm laser pulse at 4 °C. The spectra obtained at 9.7, 19.4, 29.1, 67.9, 155.2, 446.2, and 892.4 ms and 5, 9, and 18 s after the irradiation are displayed (curves 2−11, respectively). Approximately 20% (1.5 μM) of total rhodopsin was activated by a single laser flash. Inset: Difference spectra (curves 2′−11′) calculated by subtracting the spectrum recorded before irradiation (curve 1) from the spectra recorded at selected times afterward (curves 2−11). (B) Two b-spectra (curves 1 and 2) calculated from the spectral change shown in Figure 2A and the difference spectrum between lumi and meta-I (curve a, broken curve). Curves 1 and 2 represent the first and second b-spectra, respectively. Curve a was calculated from the lumi and meta-I spectra obtained from the low-temperature spectroscopy (*25*). Inset: Difference spectrum between the first and second b-spectra calculated after normalizing the absorbance at >565 nm, which reflected the spectral component of meta-Ib.

changes are shown in the inset of Figure 2A, where these changes are expressed as the difference spectra (curves 2′−11′ in the inset of Figure 2A) calculated by subtracting curve 1 from curves 2−11 in Figure 2A. The spectral changes were analyzed by using singular value decomposition (SVD) and the global fitting method, and we found that they expressed two exponential reactions (Figure 2B).

The time constant of the first component was calculated to be 13 ± 3 ms by the methods described above. However, the value is too short to be precisely determined by our experimental setup with the time resolution of 9.7 ms. Thus we estimated the time constant to be about 10 ms. The corresponding spectrum (b1-spectrum) exhibited positive and negative peaks at 440 and 515 nm, respectively (curve 1 in Figure 2B). This spectrum differs in shape from the lumi to meta-I difference spectrum having positive and negative peaks at 450 and 530 nm, respectively (curve a in Figure 2B), which was calculated from the spectra obtained by conventional low-temperature spectroscopy at −80 °C (*25*) after correcting the temperature-dependent changes of the spectral shapes of intermediate assuming that these are identical with that of original rhodopsin (*23*). In addition, a small amount of absorbance at 380 nm of the b1-spectrum suggests that no intermediate having a deprotonated Schiff base (e.g., meta-II) is formed in this reaction. On the other hand, the second component (b2-spectrum) shows positive and negative peaks at 380 and 478 nm, respectively (curve 2 in Figure 2B), indicating that this spectrum exhibits the formation process of meta-II. The time constant of this reaction is 538 ± 15 ms, which is similar to that reported in previous studies (*26*). From these results, we conclude that the first component mainly demonstrates the conversion process from meta-Ia to meta-Ib and that the second component mainly demonstrates the conversion process from meta-Ib to meta-II. The absorption maximum of meta-Ib was further calculated from the difference spectrum between meta-Ib and meta-II (Figure 2B, inset), which was obtained by the methods described by Tachibanaki et al. (*14*). The resulting value is 470 ± 1.5 nm, which is consistent with the value previously reported (*14*).

To investigate the effect of Gt on the formation processes of meta-Ib and meta-II, we prepared two samples in addition to the sample containing only rhodopsin. One of these two contains rhodopsin and Gt (sample T), and the other contains rhodopsin, Gt, and GTPγS (sample G). The sample containing only rhodopsin is denoted as sample R. The spectral changes of these samples were measured after irradiation, similar to the method described above. We then compared the spectra obtained at selected times after the irradiation of the samples. One is those obtained 67.9 ms after the irradiation and the other is those obtained 18 s after the irradiation. The former reflects the formation of meta-Ib and the latter the formation of meta-II.

The spectrum obtained 67.9 ms after irradiation of sample T (curve T1 in Figure 3A) exhibited a larger absorbance at about 465 nm when compared to the spectrum obtained from sample R (curve R1 in Figure 3A). The large absorbance at about 465 nm originates from accumulation of the meta-Ib, and therefore, this observation indicates the transient stabilization of meta-Ib in the presence of Gt. The spectrum recorded at 18 s after irradiation of sample T (curve T2 in Figure 3A) exhibited an absorbance at 380 nm due to the formation of meta II larger than that of the spectrum obtained from sample R (curve R2 in Figure 3A), indicating that an excess amount of meta II was accumulated in the presence of Gt. These results indicate that Gt interacts with both meta-Ib and meta-II and, hence, changes the thermal behavior of the intermediates. The addition of GTPγS abolished the excess formation of meta-II but not the transient stabilization of meta-Ib by Gt. Namely, the spectrum obtained at 67.9 ms after the irradiation (curve G1 in Figure 3A) was the same in shape as that obtained in the *presence* of Gt (curve T1 in Figure 3A), while that recorded at 18 s after the irradiation (curve G2 in Figure 3A) was the same in shape as that recorded in the *absence* of Gt (curve R2 in Figure 3A).

To analyze the interaction modes of Gt with these two intermediates kinetically, we plotted the changes in absorbance at 465 nm as functions of the incubation time after irradiation (Figure 3B). In comparison with sample R that contains only rhodopsin (broken curve in Figure 3B), the time profile of sample T that contains rhodopsin and Gt (solid curve in Figure 3B) showed larger positive absorbance up to 1 s incubation and larger negative absorbance after 1 s. The former change is due to the transient stabilization of

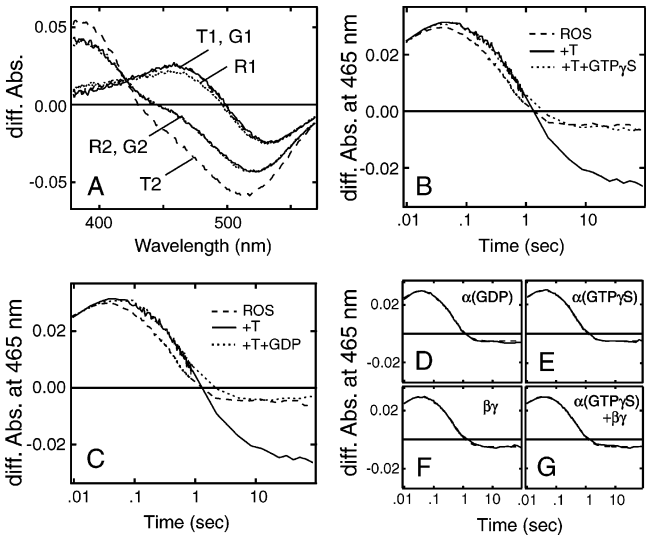

FIGURE 3: Effects of Gt, GDP, and GTPγS on the thermal behavior of meta-Ib and meta-II. (A) Effects of Gt and GTPγS on the spectra recorded at 67.9 ms and 18 s after irradiation of rhodopsin in ROS with a 532 nm laser pulse at 4 °C. The difference spectra are calculated by subtracting the spectra recorded before irradiation from those recorded after 67.9 ms (curves R1, T1, and G1) and 18 s (curves R2, T2, and G2) incubation. Curves R1 and R2 (dotted curves) are obtained from the sample containing only rhodopsin (7.5 μM). Curves T1 and T2 (broken curves) are obtained from the sample containing rhodopsin (7.5 μM) + Gt (8.1 μM). Curves G1 and G2 (solid curves) are obtained from the sample containing rhodopsin (7.5 μM) + Gt (8.1 μM) + GTPγS (200 μM). (B) Effects of Gt and GTPγS on the kinetics of meta-Ib and meta-II. Absorbance changes at 465 nm during incubation after irradiation of the samples containing rhodopsin (broken curve), rhodopsin + Gt (solid curve), and rhodopsin + Gt + GTPγS (dotted curve) are plotted as a function of the time monitored. (C) Effects of Gt and GDP on the kinetics of meta-Ib and meta-II. Absorbance changes at 465 nm of the sample containing rhodopsin (broken curve), rhodopsin + Gt (solid curve), and rhodopsin + Gt + GDP (200 μM) (dotted curve) are plotted as a function of the time monitored. (D−G) Effects of Gt subunits on the kinetics of meta-Ib and meta-II. Absorbance changes at 465 nm during incubation of the irradiated samples containing rhodopsin + Gtα(GDP) (8.1 μM) (D), rhodopsin + Gtα(GTPγS) (8.1 μM) (E), rhodopsin + Gt$\beta\gamma$ (8.1 μM) (F), and rhodopsin + Gtα(GTPγS) + Gt$\beta\gamma$ (8.1 μM) (G) are plotted as a function of the time monitored. The time course of the sample containing only rhodopsin (broken curve) is overwritten on all panels as a control.

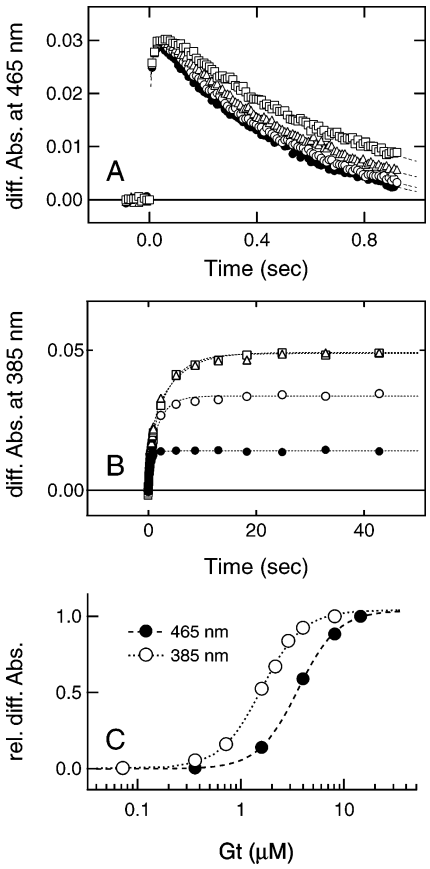

FIGURE 4: Effects of Gt concentration on the decay and formation of meta-Ib and meta-II, respectively. (A) Time courses at 465 nm (due to the decay of meta-Ib) of the sample containing rhodopsin (pH 7) + GDP (200 μM) with increasing Gt concentration [0 (solid circles), 1.6 (open circles), 4.0 (open triangles), and 8.1 (open squares) μM]. (B) Time courses at 385 nm (due to the formation of meta-II) of the sample containing rhodopsin (pH 8) with increasing Gt concentration [0 (solid circles), 1.6 (open circles), 4.0 (open triangles), and 8.1 (open squares) μM]. (C) The increase in absorbance at 465 nm at 67.9 ms due to the transient stabilization of meta-Ib (solid circles) and that at 385 nm at 18 s due to the formation of extra-meta-II (open circles) are plotted as functions of the Gt concentration in the samples. The difference in absorbance between the samples containing Gt and the sample containing only rhodopsin is calculated.

meta-Ib and the latter to the formation of extra-meta-II. The formation of extra-meta-II was abolished by the addition of GTPγS (sample G), where only the larger absorbance up to 1 s incubation, which reflects the transient stabilization of meta-Ib, was observed (dotted curve in Figure 3B). These results are consistent with those obtained at 0 to −35 °C by low-temperature time-resolved spectroscopy using the detergent-solubilized rhodopsin−glycerol sample (*13*−*15*). Therefore, we can conclude that the interaction of meta-Ib with Gt can be observed even in the physiologically relevant ROS sample at 4 °C.

Binding of Meta-Ib to GDP-Bound Gt. It has been reported that, like GTP and GTPγS, GDP can also abolish the accumulation of extra-meta-II (*12*). It is therefore of interest to investigate whether GDP can affect the binding characteristics of meta-Ib to Gt. Figure 3C shows that the addition of GDP to the sample containing rhodopsin and Gt abolished extra-meta-II formation but did not affect the transient stabilization of meta-Ib by Gt. According to these results, meta-Ib is clearly shown to bind to Gt in a different manner than that of meta-II.

We next examined whether the different Gt subunit types could interact with rhodopsin intermediates (Figure 3D−G). The results showed that none of them stabilized meta-Ib or meta-II, indicating that both the transient stabilization of meta-Ib and the formation of extra-meta-II require the trimeric form of Gt (Gtα-GDP and Gt$\beta\gamma$).

Comparison of the Binding Affinity between Meta-Ib and Meta-II to Gt. We studied the effect of Gt concentration on its interactions with meta-Ib and meta-II in order to distinguish the difference between these two binding states. Panels A and B of Figure 4 show the time courses of the absorbance changes at 465 and 385 nm in the presence of different Gt amounts. We observed that the interactions of Gt with meta-Ib and meta-II increase their absorbance at 465 and 385 nm, respectively. Their absorbances are plotted as functions of the Gt concentration in the sample (Figure 4C) and were analyzed with the equation:

$$\Delta A = -\frac{\Delta A_{max}}{1 + (EC_{50}/[Gt])^{n_H}}$$

where ΔA and ΔA_{max} are the increment and maximum increment in absorbance at 465 or 385 nm, respectively, EC_{50} is the concentration that produces half-saturation, and [Gt] and n_H are the Gt concentrations added to the sample and Hill coefficient, respectively.

The EC_{50} value for the interaction with meta-Ib is 3.2 μM with a Hill coefficient of 2.3, and the EC_{50} with meta-II is 1.6 μM with a Hill coefficient of 2.2. These results indicate that the affinity of meta-II for Gt is higher than that of meta-Ib, accounting for the formation of extra-meta-II in the equilibrium state, even in the presence of an interaction between meta-Ib and Gt.

Presence of Meta-Ib at 37 °C. To evaluate the physiological contribution of meta-Ib to the Gt activation process, we measured the equilibrium state spectra at different temperatures, from 0 to 37 °C, and investigated how much meta-Ib was present in the equilibrium mixture at physiological temperatures.

Figure 5A shows the absorbance time profiles at 465 nm for different temperatures. As already shown in Figure 2, meta-Ia (a quasi-equilibrium state of meta-Ia and lumi) converts to meta-Ib (a quasi-equilibrium state of meta-Ia and Ib) with a time constant of about 10 ms at 4 °C. The spectrophotometer cannot resolve the conversion at higher temperatures because it occurs too quickly. The decrease in absorbance at 465 nm reflects the conversion from meta-Ib to meta-II. The conversion time constants at various temperatures are listed in Table 1.

An equilibrium state among meta-Ia, meta-Ib, and meta-II was reached after the absorbance decrease at 465 nm due to the conversion from meta-Ib to meta-II. An increase in absorbance due to the formation of meta-III was then observed. The time profiles given in Figure 5A indicated that the equilibrium states were formed during the time period from 1 to 5 s after irradiation at various temperatures ranging from 4 to 37 °C. Figure 5B shows the difference spectra between the equilibrium states and original rhodopsins, and Figure 5C shows the spectra of the equilibrium states at various temperatures. We estimated the intermediate amounts in the equilibrium state by fitting the spectrum of the equilibrium state with the spectra of these intermediates. It should be noted that meta-Ib is present in the equilibrium mixture at 37 °C (Figure 5C), suggesting the physiological contribution of meta-Ib to signal transduction on the ROS membrane.

Using these intermediate amounts in the equilibrium states, the K_{eq}s among meta-Ia, meta-Ib, and meta-II at different temperatures were calculated (Table 1). In Figure 5D, the estimated equilibrium constants between the three intermediates were plotted against the reciprocal of the temperature ($1/T$). The thermodynamic parameters can then be determined by the van't Hoff equations:

$$\Delta H = -R\, d(\ln K)/d(1/T)$$

$$\Delta G = -RT \ln K$$

$$\ln K = -\Delta H/RT + \Delta S/R$$

where ΔH, ΔG, ΔS, K, R, and T are the change in enthalpy, change in free energy, change in entropy, equilibrium constant, gas constant, and temperature, respectively.

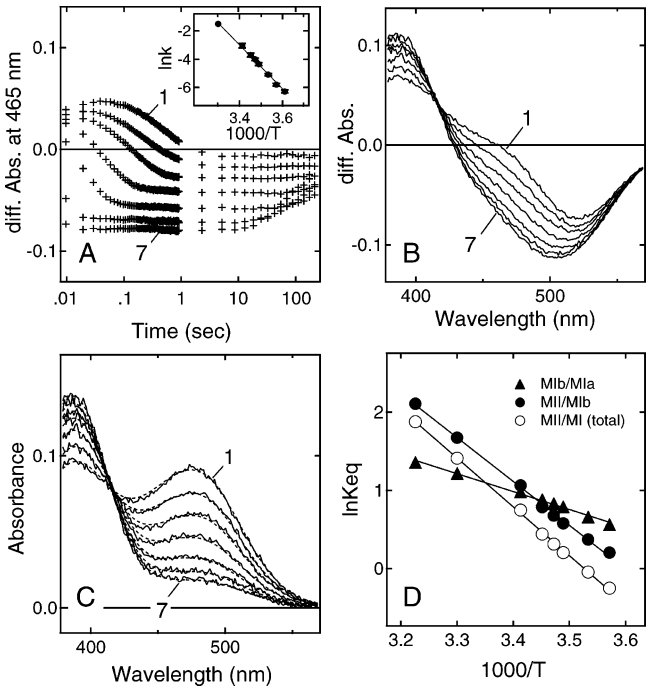

FIGURE 5: Estimation of the amounts of meta-Ib and meta-II in the equilibrium mixture produced by irradiation of rhodopsin with a 532 nm laser pulse at 0−37 °C. (A) Temperature dependence of the time course of absorbance changes at 465 nm at 4, 7, 10, 15, 20, 30, and 37 °C (plots 1−7), respectively (pH 7.0). Time constants derived from exponential fitting curves are listed in Table 1. Inset: Arrhenius plot for the observed decay rate constant of meta-Ib. The decay rate constant at 30 °C is estimated by extrapolation of the values calculated below 20 °C. (B) Difference spectra calculated by subtracting the spectra recorded before irradiation from those recorded after reaching equilibrium at each temperature (curves 1−7). (C) Absolute spectra of meta-I and meta-II in the equilibrium state at each temperature (curves 1−7) calculated by subtracting the rhodopsin and isorhodopsin spectra from the difference spectra shown in Figure 5B. The broken smooth curves are the fit curves of the three absolute spectrum approximations (see text). (D) Van't Hoff plot of the equilibrium constants. Equilibrium constants of meta-Ia/meta-Ib (solid triangles), meta-Ib/meta-II (solid circles), and the total amount of meta-I/meta-II (open circles) are plotted against the reciprocals of the temperature at which they were estimated.

Table 1: Meta-II Formation Time Constants and Equilibrium Constants Derived from Kinetic and Equilibrium Data[a]

temp (°C)	τ (ms)	K_{eq}(MIb/MIa)	K_{eq}(MII/MIb)	% MIb
4	538 (15)	1.65	1.03	37.9
7	343 (10)	1.75	1.22	35.8
10	164 (5)	1.94	1.45	33.7
15	55 (4)	2.3	1.96	29.5
20	19 (2)	2.67	2.9	23.4
30	6 (1)[b]	3.37	5.32	15.1
37	0.7 (0.2)[b]	3.89	8.25	10.5

[a] Time constant (τ) values were obtained from the exponential analysis of the spectral change due to meta-I decay and meta-II formation. Equilibrium constants were obtained from the spectral separation analysis (see text) of the spectra of the equilibrium states among meta-Ia, meta-Ib, and meta-II (Figure 5C). The values in parentheses are estimated standard deviations. [b] τ values at 30 and 37 °C were obtained from extrapolation of the τ values of 4−20 °C.

The calculated ΔH values are $\Delta H_{MIb/MIa} = 4.6 \pm 0.2$ kcal/mol and $\Delta H_{MII/MIb} = 11.2 \pm 0.2$ kcal/mol. If we consider a mixture of meta-Ia and meta-Ib as a single component (meta-I), we then have $\Delta H_{MII/MI-total} = 12.4 \pm 0.4$ kcal/mol and $\Delta S = 43.8 \pm 0.6$ cal mol^{-1} deg^{-1}, which are similar to the

Scheme 1

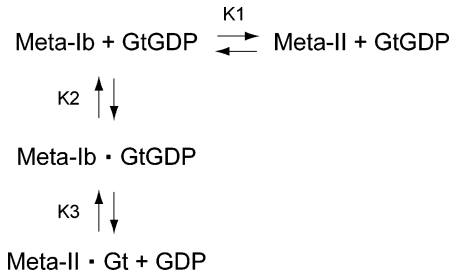

values that were previously reported using the ROS (*27*, *28*) and detergent-solubilized (*8*, *29*) conditions.

DISCUSSION

In the present study, we used a CCD spectrophotometer to demonstrate that meta-Ib was detected in a physiologically relevant ROS sample at 37 °C. We also demonstrated that meta-Ib binds to the GDP-bound Gt, a physiological form of Gt. The EC_{50} value of meta-Ib binding to Gt is two times larger than that of meta-II binding to Gt, while the Hill coefficients are about 2 in both cases. On the basis of these findings, we discuss the binding mechanism of meta-Ib and its physiological role in Gt activation.

Binding to Gt Prior to the Deprotonation of the Schiff Base Chromophore. In vertebrate phototransduction, meta-II formation has been thought to be crucial in the binding to Gt and inducing a GDP−GTP exchange reaction on the α-subunit of Gt (activation of Gt). Because it is the intermediate that has a deprotonated Schiff base chromophore, loss of the electrostatic interaction between the Schiff base and the Glu113 counterion through a proton transfer has been considered to be important for the binding and activation of Gt (*30*). On the other hand, we found that meta-Ib, the precursor of meta-II, can bind to Gt prior to meta-II formation, though it cannot induce the exchange reaction on the α-subunit of Gt. These findings strongly suggest that the interaction between photoactivated rhodopsin and Gt can occur regardless of the existence of the proton at the Schiff base. That is, the deprotonation of the Schiff base is not directly related to the binding of the rhodopsin intermediate to Gt.

By using the engineered cross-linkages, it was demonstrated that meta-II has the protein structure that is created by the separation of the cytoplasmic ends of helices III and VI (*31*, *32*), while the preceding protonated intermediate does not have a similar arrangement (*33*). Combined with our results, it is suggested that the massive helical rearrangement is not necessary for the binding of the rhodopsin intermediate to Gt but is essential for the GDP−GTP exchange reaction on Gt. In this sense, meta-Ib can be regarded as "the Gt binding state with minimum helix rearrangement" (*34*) and meta-II as "the active state with massive helix rearrangement" (*31*).

As previously described, the addition of excess GDP to the sample completely inhibited the formation of extra-meta-II, whereas it does not perturb the binding of Gt to meta-Ib (Figure 3C). These results indicate that Gt forming a complex with meta-II has no GDP in its nucleotide binding site, while that forming a complex with meta-Ib is in a GDP-bound form. Thus, we first thought that Scheme 1 could account

Scheme 2

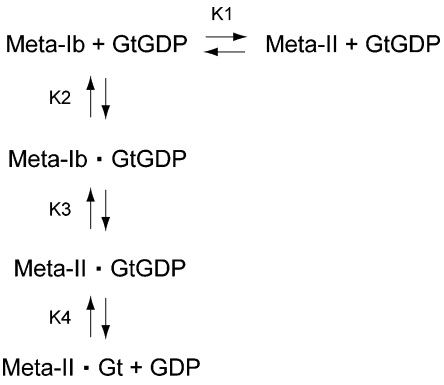

Scheme 3

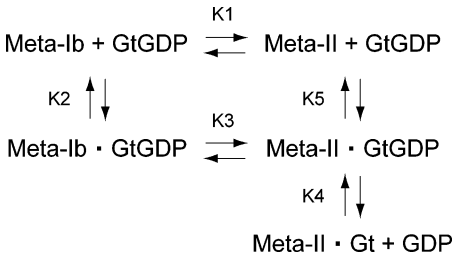

for the experimental facts. In Scheme 1 K_n ($n = 1, 2, 3, ...$) are the equilibrium constants.

From Scheme 1, it was expected that the addition of excess GDP caused the shift of the equilibrium between meta-Ib·GtGDP and meta-II·Gt + GDP toward meta-Ib·GtGDP, resulting in accumulation of the species having visible absorption spectra (meta-Ib and meta-Ib·GtGDP) in the equilibrium. More importantly, this equilibrium state should contain the visible-absorbing species more than the equilibrium state in the absence of Gt and GDP does, because the equilibrium in the presence of Gt and an excess amount of GDP contains the state meta-Ib·GtGDP which is not present in the equilibrium in the absence of Gt and GDP. However, despite our extensive efforts of changing Gt and/or GDP concentrations in the sample, we could not detect a measurable difference in the spectrum between these two states. These results lead us to speculate that the meta-Ib·GtGDP should be in equilibrium with a complex expressing meta-II·GtGDP, which also forms in equilibrium with meta-II-Gt + GDP, and the reaction scheme should fulfill one of the following two conditions: (1) The equilibrium constants K_1 and K_3 should be identical (Scheme 2). (2) Meta-II·GtGDP and meta-II + GtGDP should be mutually convertible with equilibrium constant K_5, and $K_2 = K_5$ (Scheme 3).

At present, we do not have any experimental evidence about which reaction scheme is true. Therefore, we combined these two schemes into Scheme 4. Meta-II forming a complex with GDP-bound Gt (meta-II−Gt·GDP, Scheme 4) should have a protein structure different from that of meta-II−Gt (extra-meta-II), although they have similar absorption maxima. Characterization of these two states would be important for furthering our understanding of the Gt activation mechanism by rhodopsin. In this context, there are reported two meta-II states which are identical in absorption spectrum but are different in protein structure. These states were named meta-IIa and meta-IIb, which are distinguished by the protonation state of glutamic acid at position 134

Scheme 4

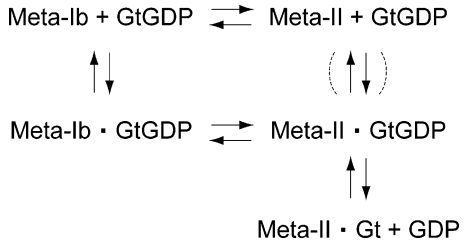

(Glu134), resulting in different protein conformations (*35*). Meta-IIb is formed from meta-IIa by the protonation of the glutamic acid and it is the state that forms the extra-meta-II, while meta-IIa is the state that does not interact with Gt. Therefore, these two states may not be the same as the states described above, but detailed investigation should provide insight into the Gt activation mechanism by rhodopsin.

Our results clearly showed that meta-Ib forms a complex with GDP-bound Gt. If meta-Ib is the only state that can form a complex with GDP-bound Gt, the process of Gt activation should proceed through at least three steps: the first is the binding of meta-Ib to GDP-bound Gt, the second is the conversion of meta-Ib to meta-II in the complex, and the third is the conversion to another form of meta-II with release of GDP from the complex. The meta-II−Gt complex is then bound to GTP, followed by dissociation into meta-IIb and the α- and $\beta\gamma$-subunits of Gt. For activation of the next GDP-bound Gt, the meta-IIb that dissociates from Gt should convert to meta-Ib. In our kinetic analyses, the time constant for the reverse reaction from meta-II to meta-Ib at 37 °C was estimated to be 5.8 ms by multiplying the apparent time constant and the equilibrium constant at 37 °C shown in Table 1. The apparent time constant at 37 °C was estimated by extrapolation of the time constants calculated from the data obtained over the temperature range from 0 to 20 °C. Considering that the amount of meta-Ib present under the equilibrium conditions at 37 °C is about 10% and the theoretical limit of the R*−Gt·GDP encounter rate is 7000 s^{-1} (*36*), the meta-Ib−Gt·GDP encounter rate might be in the range of 150 Gt*/s. On the other hand, the maximal rate for Gt activation was estimated to range from ∼120 Gt*/s per R* by biochemical measurement (*37*) to >1300 Gt*/s per R* by light scattering measurement (*38*, *39*). If we attempt to explain the higher rates obtained from light scattering measurements, it is appropriate to consider that GDP-bound Gt can bind not only to meta-Ib but also to meta-II (Scheme 4).

Comparison of the Gt Binding Characteristics of Meta-Ib and Meta-II. To quantitatively compare the binding affinity to Gt between meta-Ib and meta-II, we calculated the EC_{50} values of the binding of these intermediates to Gt from the experimental results that are shown in Figure 4. The meta-Ib and meta-II EC_{50} values are 3.2 and 1.6 μM, respectively. The difference in affinity between these intermediates could cause an equilibrium shift toward meta-II in the presence of Gt, even though meta-Ib also has the ability to bind to Gt.

It should be noted that the EC_{50} values of these intermediates are different from each other, indicating the different characteristics of their binding sites. We previously reported that meta-Ib binds to the C-terminus of Gtα in a manner different from that of meta-II (*15*). This means that only one of the two leucines located at the C-terminus of Gtα is needed for binding to meta-Ib; however, both leucines are required for binding to meta-II. These differences demonstrate that the binding affinity of meta-II is higher than that of meta-Ib. It was also reported that the C-terminus of Gtγ interacts with meta-II (*40*, *41*). The fact that meta-Ib exhibits the same Hill coefficient as meta-II therefore suggests that the C-terminus of Gtγ also interacts with meta-Ib, although the values of Hill coefficients do not tell how many Gt subunits participate in binding with rhodopsin intermediates.

In conclusion, we have identified meta-Ib, the binding state of GDP-bound Gt, under physiologically relevant conditions. To our knowledge, this is the first time to identify the binding state of GDP-bound G protein in the rhodopsin system as well as other GPCR systems that are activated by diffusible agonist ligand. Therefore, the elucidation of the binding mechanism of meta-Ib to G protein will give valuable information about, for example, the dynamic mechanism of G-protein activation in a rhodopsin system as well as a typical GPCR system.

ACKNOWLEDGMENT

We thank Drs. Shuji Tachibanaki, Akihisa Terakita, and Takahiro Yamashita for helpful discussions.

REFERENCES

1. Wald, G. (1968) Molecular basis of visual excitation, *Science 162*, 230−239.
2. Hubbard, R., and Kropf, A. (1958) The action of light on rhodopsin, *Proc. Natl. Acad. Sci. U.S.A. 44*, 130−139.
3. Yoshizawa, T., and Wald, G. (1963) Pre-lumirhodopsin and the bleaching of visual pigments, *Nature 197*, 1279−1286.
4. Shichida, Y., and Imai, H. (1998) Visual pigment: G-protein-coupled receptor for light signals, *Cell. Mol. Life Sci. 54*, 1299−1315.
5. Stryer, L. (1986) Cyclic GMP cascade of vision, *Annu. Rev. Neurosci. 9*, 87−119.
6. Gilman, A. G. (1987) G proteins: transducers of receptor-generated signals, *Annu. Rev. Biochem. 56*, 615−649.
7. Han, M., Lou, J., Nakanishi, K., Sakmar, T. P., and Smith, S. O. (1997) Partial agonist activity of 11-cis-retinal in rhodopsin mutants, *J. Biol. Chem. 272*, 23081−23085.
8. Matthews, R. G., Hubbard, R., Brown, P. K., and Wald, G. (1963) Tautomeric form of metarhodopsin, *J. Gen. Physiol. 47*, 215−240.
9. Hofmann, K. P. (1985) Effect of GTP on the rhodopsin-G-protein complex by transient formation of extra metarhodopsin II, *Biochim. Biophys. Acta 810*, 278−281.
10. Bennett, N., Michel-Villaz, M., and Kuhn, H. (1982) Light-induced interaction between rhodopsin and the GTP-binding protein. Metarhodopsin II is the major photoproduct involved, *Eur. J. Biochem. 127*, 97−103.
11. Emeis, D., Kuhn, H., Reichert, J., and Hofmann, K. P. (1982) Complex formation between metarhodopsin II and GTP-binding protein in bovine photoreceptor membranes leads to a shift of the photoproduct equilibrium, *FEBS Lett. 143*, 29−34.
12. Kahlert, M., Konig, B., and Hofmann, K. P. (1990) Displacement of rhodopsin by GDP from three-loop interaction with transducin depends critically on the diphosphate beta-position, *J. Biol. Chem. 265*, 18928−18932.
13. Tachibanaki, S., Imai, H., Mizukami, T., Okada, T., Imamoto, Y., Matsuda, T., Fukada, Y., Terakita, A., and Shichida, Y. (1997) Presence of two rhodopsin intermediates responsible for transducin activation, *Biochemistry 36*, 14173−14180.
14. Tachibanaki, S., Imai, H., Terakita, A., and Shichida, Y. (1998) Identification of a new intermediate state that binds but not activates transducin in the bleaching process of bovine rhodopsin, *FEBS Lett. 425*, 126−130.
15. Morizumi, T., Imai, H., and Shichida, Y. (2003) Two-step mechanism of interaction of rhodopsin intermediates with the C-terminal region of the transducin alpha-subunit, *J. Biochem. (Tokyo) 134*, 259−267.

16. Papermaster, D. S., and Dreyer, W. J. (1974) Rhodopsin content in the outer segment membranes of bovine and frog retinal rods, *Biochemistry 13*, 2438−2444.
17. Shichi, H., and Somers, R. L. (1978) Light-dependent phosphorylation of rhodopsin. Purification and properties of rhodopsin kinase, *J. Biol. Chem. 253*, 7040−7046.
18. Fukada, Y., Matsuda, T., Kokame, K., Takao, T., Shimonishi, Y., Akino, T., and Yoshizawa, T. (1994) Effects of carboxyl methylation of photoreceptor G protein gamma-subunit in visual transduction, *J. Biol. Chem. 269*, 5163−5170.
19. Phillips and Cerione (1988) The intrinsic fluorescence of the alpha subunit of transducin. Measurement of receptor-dependent guanine nucleotide exchange, *J. Biol. Chem. 263*, 15498−15505.
20. Fahmy, K., and Sakmar, T. P. (1993) Regulation of the rhodopsin-transducin interaction by a highly conserved carboxylic acid group, *Biochemistry 32*, 7229−7236.
21. Lamb, T. D. (1995) Photoreceptor spectral sensitivities: common shape in the long-wavelength region, *Vision Res. 35*, 3083−3091.
22. Govardovskii, V. I., Fyhrquist, N., Reuter, T., Kuzmin, D. G., and Donner, K. (2000) In search of the visual pigment template, *Visual Neurosci. 17*, 509−528.
23. Imai, H., Mizukami, T., Imamoto, Y., and Shichida, Y. (1994) Direct observation of the thermal equilibria among lumirhodopsin, metarhodopsin I, and metarhodopsin II in chicken rhodopsin, *Biochemistry 33*, 14351−14358.
24. Applebury, M. L. (1984) Dynamic processes of visual transduction, *Vision Res. 24*, 1445−1454.
25. Shichida, Y., Kandori, H., Okada, T., Yoshizawa, T., Nakashima, N., and Yoshihara, K. (1991) Differences in the photobleaching process between 7-cis- and 11-cis-rhodopsins: a unique interaction change between the chromophore and the protein during the lumi-meta I transition, *Biochemistry 30*, 5918−5926.
26. Parkes, J. H., and Liebman, P. A. (1984) Temperature and pH dependence of the metarhodopsin I-metarhodopsin II kinetics and equilibria in bovine rod disk membrane suspensions, *Biochemistry 23*, 5054−5061.
27. Cooper, A. (1981) Rhodopsin photoenergetics: lumirhodopsin and the complete energy profile, *FEBS Lett. 123*, 324−326.
28. Thorgeirsson, T. E., Lewis, J. W., Wallace-Williams, S. E., and Kliger, D. S. (1993) Effects of temperature on rhodopsin photointermediates from lumirhodopsin to metarhodopsin II, *Biochemistry 32*, 13861−13872.
29. Arnis, S., and Hofmann, K. P. (1993) Two different forms of metarhodopsin II: Schiff base deprotonation precedes proton uptake and signaling state, *Proc. Natl. Acad. Sci. U.S.A. 90*, 7849−7853.
30. Robinson, P. R., Cohen, G. B., Zhukovsky, E. A., and Oprian, D. D. (1992) Constitutively active mutants of rhodopsin, *Neuron 9*, 719−725.
31. Farrens, D. L., Altenbach, C., Yang, K., Hubbell, W. L., and Khorana, H. G. (1996) Requirement of rigid-body motion of transmembrane helices for light activation of rhodopsin, *Science 274*, 768−770.
32. Sheikh, S. P., Zvyaga, T. A., Lichtarge, O., Sakmar, T. P., and Bourne, H. R. (1996) Rhodopsin activation blocked by metal-ion-binding sites linking transmembrane helices C and F, *Nature 383*, 347−350.
33. Resek, J. F., Farahbakhsh, Z. T., Hubbell, W. L., and Khorana, H. G. (1993) Formation of the meta II photointermediate is accompanied by conformational changes in the cytoplasmic surface of rhodopsin, *Biochemistry 32*, 12025−12032.
34. Ruprecht, J. J., Mielke, T., Vogel, R., Villa, C., and Schertler, G. F. (2004) Electron crystallography reveals the structure of metarhodopsin I, *EMBO J. 23*, 3609−3620.
35. Arnis, S., Fahmy, K., Hofmann, K. P., and Sakmar, T. P. (1994) A conserved carboxylic acid group mediates light-dependent proton uptake and signaling by rhodopsin, *J. Biol. Chem. 269*, 23879−23881.
36. Pugh, E. N., Jr., and Lamb, T. D. (1993) Amplification and kinetics of the activation steps in phototransduction, *Biochim. Biophys. Acta 1141*, 111−149.
37. Leskov, I. B., Klenchin, V. A., Handy, J. W., Whitlock, G. G., Govardovskii, V. I., Bownds, M. D., Lamb, T. D., Pugh, E. N., Jr., and Arshavsky, V. Y. (2000) The gain of rod phototransduction: reconciliation of biochemical and electrophysiological measurements, *Neuron 27*, 525−537.
38. Kahlert, M., and Hofmann, K. P. (1991) Reaction rate and collisional efficiency of the rhodopsin-transducin system in intact retinal rods, *Biophys. J. 59*, 375−386.
39. Heck, M., and Hofmann, K. P. (2001) Maximal rate and nucleotide dependence of rhodopsin-catalyzed transducin activation: initial rate analysis based on a double displacement mechanism, *J. Biol. Chem. 276*, 10000−10009.
40. Yan, E. C., Kazmi, M. A., Ganim, Z., Hou, J. M., Pan, D., Chang, B. S., Sakmar, T. P., and Mathies, R. A. (2003) Retinal counterion switch in the photoactivation of the G protein-coupled receptor rhodopsin, *Proc. Natl. Acad. Sci. U.S.A. 100*, 9262−9267.
41. Matsuda, T., Hashimoto, Y., Ueda, H., Asano, T., Matsuura, Y., Doi, T., Takao, T., Shimonishi, Y., and Fukada, Y. (1998) Specific isoprenyl group linked to transducin gamma-subunit is a determinant of its unique signaling properties among G-proteins, *Biochemistry 37*, 9843−9850.
42. Haga, K., Haga, T., and Ichiyama, A. (1986) Reconstitution of the muscarinic acetylcholine receptor. Guanine nucleotide-sensitive high affinity binding of agonists to purified muscarinic receptors reconstituted with GTP-binding proteins (Gi and Go), *J. Biol. Chem. 261*, 10133−10140.
43. Shichida, Y., Matuoka, S., and Yoshizawa, T. (1984) Formation of photorhodopsin, a precursor of bathorhodopsin, detected by picosecond laser photolysis at room temperature, *Photobiochem. Photobiophys. 7*, 221−228.
44. Schoenlein, R. W., Peteanu, L. A., Mathies, R. A., and Shank, C. V. (1991) The first step in vision: femtosecond isomerization of rhodopsin, *Science 254*, 412−415.
45. Hug, S. J., Lewis, J. W., Einterz, C. M., Thorgeirsson, T. E., and Kliger, D. S. (1990) Nanosecond photolysis of rhodopsin: evidence for a new, blue-shifted intermediate, *Biochemistry 29*, 1475−1485.
46. Yoshizawa, T., and Shichida, Y. (1982) Low-temperature spectrophotometry of intermediates of rhodopsin, *Methods Enzymol. 81*, 333−354.

BI0504512